

RIGID GLULAM JOINTS TO CONCRETE ABUTMENTS WITH GLUED-IN STEEL RODS

Kai Simon¹, Simon Aicher²

ABSTRACT: It is reported on rigid moment and shear force resistant connections of glulam to concrete or steel abutments based on glued-in steel rods. The connections are especially meant for clamped columns and integral bridge decks and wide-span end-clamped floors. In order to prevent premature splitting failure of the joint and to enforce a rather even shear force distribution on spaced rods the issue of lateral joint reinforcement by self-tapping screws or/and glued-on plywood panels is emphasized. The proposed design equations are calibrated by results of an extensive experimental campaign, revealing that the new Eurocode EC5-1-1 is overly conservative regarding lateral forces and respective normal force interaction. It is revealed case study-wise that the investigated rigid joint configurations present superior rotational stiffness and load capacities vs. today's primarily employed mechanical fastener solutions with slotted-in steel plates or grout embedment of the GLT column in bucket foundations. The study demonstrates a technically competitive and environmentally advantageous timber solution vs. precast concrete columns. It offers new options for hybrid timber-concrete applications for timber bridge decks and clamped wide-span floors.

KEYWORDS: rigid glulam connections, moment and shear force resistant joints vs. concrete abutments, lateral joint reinforcement, self-tapping screws, glued-on plywood panels, clamped columns, bridge decks and floors, hybrid timber-concrete joints

1 INTRODUCTION

Today moment and shear force resistant connections of glulam (GLT) beams to concrete abutments, mainly occurring with columns, are realized by slotted-in steel plates fixed by dowel type fasteners. In order to achieve a high rotational stiffness, the steel "swords" have to be rather long altogether with a high number of dowels (Fig. 1a). Alternatively, the GLT column foot can be directly grouted in bucket foundations (Figure 1b). Both alternatives do not represent a practical construction method in case of rigidly jointing horizontally oriented beams for a timber bridge deck or a wide-span timber floor slab (Figure 1d). Rigid joints based on glued-in steel rods cast-in or screwed to RC abutments present a powerful tool to solve this connection task. Assets beyond high load capacity and stiffness consist in high fire resistance due to the hidden steel bars, minimized corrosion potential and less/no timber durability hazard of the joint due to protection from free or condensation water. A further asset of rigidly clamped column bearings consists in the creation of frame-type construction solutions, leading to reduced efforts in bracing especially at irregular spacings of columns in open space wide-span timber floor systems.

2 TECHNICAL CHALLENGE

The potential of rigid joints in glulam and LVL by glued-in rods is evident from numerous research work, increasing numbers of use in timber construction works

and hence its consideration in the presently drafted new Eurocode 5-1-1 [1]. Today such joints are mostly used for timber to timber connections. Hybrid timber to steel joints based on glued-in rods exist (e.g. Figure 2) however are rare (e.g. [4; 5]). The assets of axially loaded steel rods glued-in parallel or inclined to wood fiber direction is widely acknowledged and sufficiently covered by commonly agreed-on design rules. However, in moment-rigid joints, e.g. at a clamped column basis lateral rod

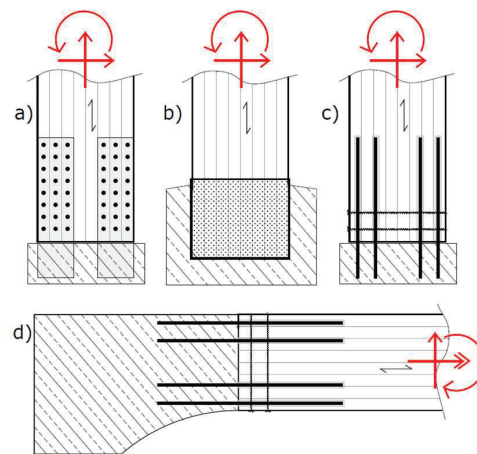


Figure 1: Rigid glulam to concrete connection alternatives a) dowelled timber steel plate joint b) joint grouted in bucket foundation c), d) glued-in steel rods with lateral reinforcement for columns (c) and bridge decks/floors (d)

¹ Kai Simon, Materials Testing Institute University of Stuttgart, kai.simon@mpa.uni-stuttgart.de

² Simon Aicher, Materials Testing Institute University of Stuttgart, Head of Department

forces resulting from shear force and torsional moment and their interaction with axial forces has to be considered, too. Lateral rod forces induce tensile stresses perpendicular to grain in the end grain area, which can lead to crack formation parallel to the rod axis at low load levels in case the rod distance to the loaded edge $a_{4,t}$ is small. The lateral force resistance of glued-in rods, as addressed now in [1], clearly represents a rather worst-case scenario of a rod positioned very close to the loaded edge. A previous more plausible and economically advantageous design approach has been dropped ([2] and [3]).

In order to prevent premature crack formation by lateral forces the joint has to be adequately reinforced perpendicular to grain. At present it is unknown which type of reinforcement is the best option and to what extent it increases the load capacity and stiffness of the joint. These questions set the frame for the reported research work which aims to provide ready to use joint construction and design solutions.

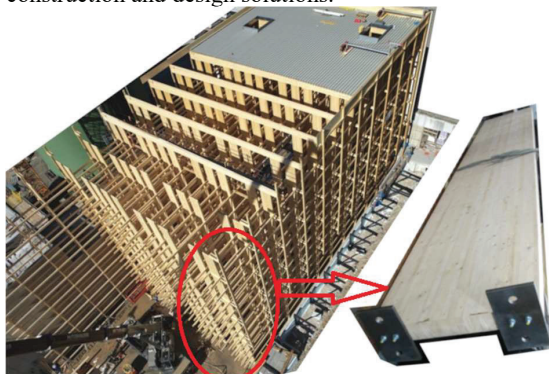


Figure 2: Example of a timber high bay racking built by Kaufmann Bausysteme GmbH, Reuthe, Austria, in 2007 consisting of clamped columns connected by glued-in steel rods [4]; the joint behaviour and capacity were verified at MPA Stuttgart.

3 GLUED-IN RODS: STATE OF THE ART

3.1 GENERAL

Research on glued-in steel rods dates back to the 1970ies [5; 6]. The investigations focussed on load capacity of the joints subjected to different loading modes and apt adhesives to enable strong and durable joints. Compilations of previous research, although not exhaustive can be found in [7]. Execution and design of glued-in rods was firstly standardized in DIN 1052:2004 [8] and DIN EN 1995-1-1/NA [9] in conjunction with nationally approved adhesives [10-13]. Based on increased knowledge and built heritage glued-in rod connections have now been incorporated in the draft of Eurocode 5-1-1 [1] referencing EN 17334 [14] with regard to testing and qualification of 2-component adhesives for glued-in rod applications.

3.2 AXIAL LOADING

The literature on axially loaded rods glued in glulam parallel to fiber is vast, e.g. [2; 6; 7; 15-17]. The latest European design proposal for axially loaded rods stated in prEN 1995-1-1 [1] is closely related to specifications given in DIN EN 1995-1-1/NA [9]. The European design equation for the characteristic axial capacity $F_{ax,Rk}$ of a single glued-in steel rod parallel to fiber with bonded-in length l_w reads

$$F_{ax,Rk} = \min \left\{ \frac{\pi \cdot d \cdot l_{w,ef} \cdot f_{w,k}}{E_s \cdot A_s \cdot \varepsilon_{u,timber}} \right\} \leq F_{t,k} \quad (1)$$

where

- d nominal diameter of the rod
- $l_{w,ef}$ effective withdrawal length as minimum of:
 l_w ; $40 \cdot d$; 1000 mm
- $f_{w,k}$ characteristic withdrawal (shear) strength of the bond line acc. to [1; 9] or e.g. Z-9.1-705 [10]
- E_s modulus of elasticity of the steel rod
- A_s nominal stress area acc. to EN ISO 898-1 for threaded rods and acc. to EN 10080 for ribbed steel bars
- $\varepsilon_{u,timber}$ failure strain of timber parallel to grain (= 2,4 % for softwood)
- $F_{t,k}$ characteristic tensile resistance of the steel rod (see [1])

Figure 3 depicts the relationship of $f_{w,k}$ with bond / withdrawal length l_w for configurations of rods bonded parallel to fiber as specified in [1; 9]. Further, test results with various slenderness rod ratios and different adhesives presented in [7] are shown.

Spacings and edge distances of axially glued-in rods are specified in [1] as $a_2 = 5 \cdot d$ and $a_{4,e} = 2.5 \cdot d$, see Figure 4.

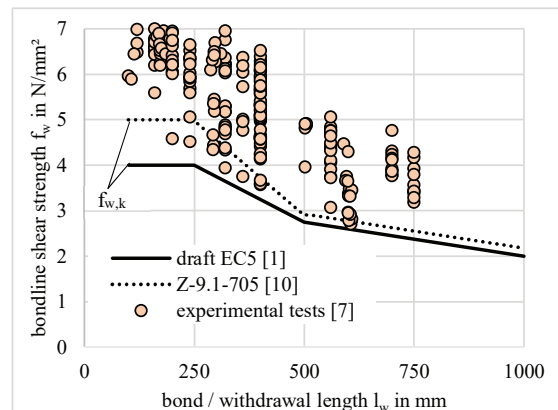


Figure 3: Bond line withdrawal / shear strength of axially loaded steel rods glued-in parallel to fiber in softwood GLT depending on withdrawal i.e. bond length l_w from test results [7] and design rules acc. to draft EC5 [1] and Technical approval [10]

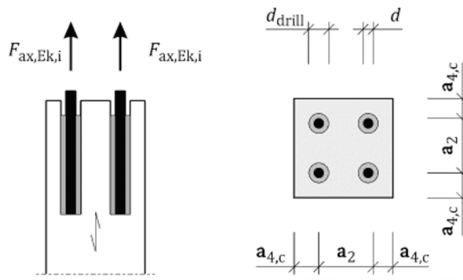


Figure 4: Notations of spacings and edge distances of axially loaded steel rods glued-in parallel to GLT fiber

3.3 LATERAL LOADING

Figure 5 shows the basic lateral force resistance behaviour as dependent on the distance to the loaded edge $a_{4,t}$ (see Figure 6) as obtained in former tests by Riberholt in 1977 [15], Möhler and Hemmer in 1981 [16] and then by Blaß and Laskewitz in 2001 [2]. The depicted results represent a test configuration of GLT with metrically threaded glued-in steel rods with a diameter d and bond length l_w of 16 mm and 320 mm ($= 20 \cdot d$), respectively. A design model by Blaß and Laskewitz [2] based on a calculation model for splitting perpendicular to grain by Ehlbeck et al. [3] which describes the increasing load carrying capacity for larger distances $a_{4,t}$ quite well (see dotted line in Figure 5), was not considered in a standard. Instead the design model presented by Riberholt in 1988 [17] was established in DIN 1052:2004 [8] and later in the German Annex of Eurocode 5 [9]. The design model is based on the Johansen yield model [18] for dowel-type steel fasteners. With regard to splitting perpendicular to grain the model stipulates a minimum distance $a_{4,t} = 4 \cdot d$ to the loaded edge but doesn't consider any capacity increase for larger edge distances. The most recent European design equations for the lateral load carrying capacity of rods glued-in GLT parallel to grain acc. to prEN 1995-1-1 are

$$F_{lat,Rk} = \min \begin{cases} d \cdot f_{h,k} \cdot \left(\sqrt{(l_h + 2e)^2 + l_h^2} - l_h - 2e \right) & (2a) \\ d \cdot f_{h,k} \cdot \left(\sqrt{e^2 + \frac{2M_{y,k}}{d \cdot f_{h,k}}} - e \right) & (2b) \end{cases}$$

where

- d nominal diameter of the glued-in rod
- l_h embedment depth ($l_h = l_w$)
- e distance between load and bond line ($e = l_{can}$)
- $M_{y,k}$ the characteristic yield moment of the rod specified as

$$M_{y,k} = 0,3 \cdot f_{u,k} \cdot d_e^{2,6} \quad (3)$$

where

- d_e the equivalent tensile stress diameter for rods with metric thread
- $f_{u,k}$ characteristic tensile strength of steel rod

and the characteristic embedment strength

$$f_{h,k} = 0,1 \cdot \frac{0,082 \cdot (1 - 0,01 \cdot d_{drill}) \cdot \rho_k}{k_{mat}} \quad (4)$$

where

- d_{drill} the drill diameter of the hole in the timber part
- $k_{mat} = k_{90} \cdot \sin^2 \alpha + \cos^2 \alpha$
- $k_{90} = 1,35 + 0,015 \cdot d$
- ρ_k characteristic density of the timber

Acc. to [1] the embedment strength for a laterally loaded bonded-in rod inserted parallel to grain should be taken as 10% of the embedment strength of a laterally loaded bonded-in rod inserted perpendicular to grain. Hence as angle α between load and fiber direction is 0° in the here considered configuration, $k_{mat} = 1$ in Eq. (4). It should be mentioned that the embedment strength $f_{h,k}$ for dowels inserted parallel to grain given in [1] is specified extremely conservative and has been significantly lowered as compared to the previous EC5 draft [19] and German Annex of EC5 [9], see below (chapter 6.1).

Spacing a_2 and edge distance $a_{4,c}$ in [1] conform to the provisions of axially loaded steel rods; $a_{4,t}$ is prescribed as $4 \cdot d$ as previously in [8], see Figure 6.

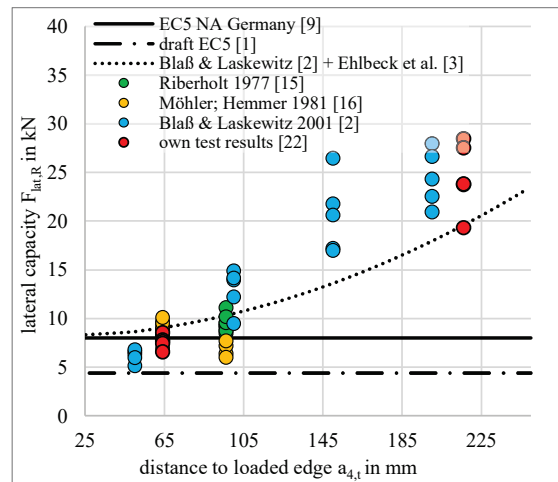


Figure 5: Lateral resistance capacity of a single rod configuration ($d_{rod} = 16$ mm, metrically threaded) glued-in parallel to grain acc. to literature [2 - 3; 15 - 16], codes [1; 9] and own experimental tests

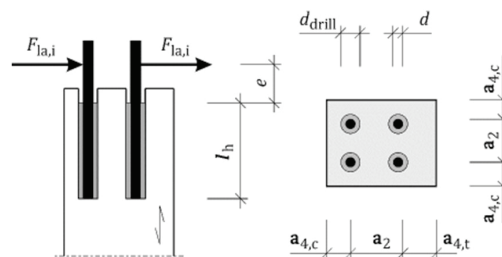


Figure 6: Spacings and distances of laterally loaded steel rods glued-in parallel to GLT fiber

4 COMBINED AXIAL AND LATERAL LOADING

For combined lateral and axial loadings acting on glued-in rods prEN1995-1-1 [1] specifies the interaction relationship:

$$\left(\frac{F_{ax,Ek}}{F_{ax,Rk}}\right)^n + \left(\frac{F_{lat,Ek}}{F_{lat,Rk}}\right)^n \leq 1,0 \quad (5)$$

where $n = 2$. It should be mentioned that the exponent n in Eq. (5) has been changed from formerly $n = 1$ in [19] to $n = 2$, as firstly proposed by Riberholt [15] and specified previously in the German Annex of EC5 [9]. The exponent of $n = 2$ was also substantiated by tests of the authors.

5 RESEARCH PROGRAM AND TEST SET-UPS

Extensive research on rigid joints of GLT to concrete foundations or steel beams / sockets by means of glued-in steel rods started at MPA in 2014 in conjunction with the development of the Stuttgart timber model bridge (STMB) (see e.g. [20; 21]).



Figure 7: Test specimen of Stuttgart Timber Model Bridge with rigid GLT to concrete connection with glued-in rebars [24]

Based on the very successful use of the rigid concrete - glulam joint in the STMB project a comprehensive research program was initiated to clarify remaining open questions of this jointing technology. Hereby especially effects of different reinforcement alternatives intended to prevent premature splitting parallel to fiber in the joint area and respective design methods were of prime interest. It is obvious that a transparent validation of the reinforcement gains necessitates as basis knowledge about the load carrying capacity of unreinforced joints inevitably, too. In the same sense it is further important to understand the reinforcement mechanisms and gains firstly at pure axial and lateral rod loading before addressing a combined loading situation as existent in any rigidly clamped reinforced connection.

The load capacities of different actions were identified via: axial tests, predominant shear force tests realized as

bending tests and cantilever tests with combined axial and lateral force action. The loading principles of the shear and cantilever tests are shown in Figure 8. It can be seen that the cantilever tests were performed with two different moment – shear force ratios of $M/V = 0,55$ and $1,15$, respectively. All mentioned loading configurations were tested unreinforced and with three different reinforcement alternatives, shown in Figure 9.

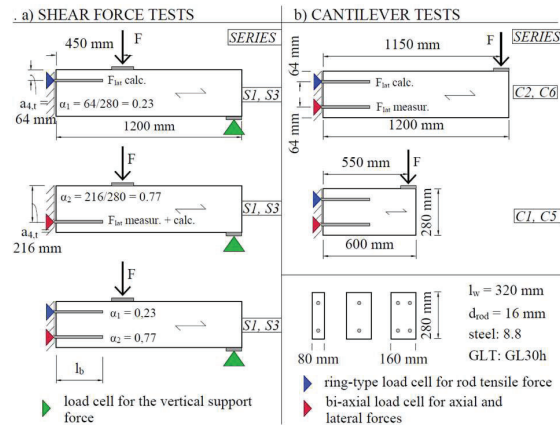


Figure 8: Overview on glued-in steel rod test configurations, a) quasi pure lateral loading; b) combined axial and lateral loading in cantilever tests

The investigated reinforcements were i) self-tapping screws ($d_{screw} = 8$ mm), ii) laterally and iii) end-grain bonded beech plywood panels with a thickness of 20 mm. Tables 1 and 2 give a condensed overview on the test program (see also [22] and [23]). In all cases the glulam (GLT) specimens were of strength class GL30h. The cross-sectional height was throughout 280 mm and widths were 80 mm and 160 mm being 5 or 10 times the steel rod diameter of $d = 16$ mm, respectively. The spacings of the steel rods were set as the minimally possible acc. to [1] and [9], being $a_{4,t} = 4 \cdot 16$ mm = 64 mm. The withdrawal length and the diameter of the drill hole in the GLT were throughout $l_w = 320$ mm ($20 \cdot d$) and $d_{drill} = 20$ mm, respectively, representing a practically relevant configuration. The distances of the screws from the end-grain face, from the width edge and from the rod were chosen (closest possible) as $a_{3,CG} = 28$ mm, $a_{4,CG} = 20$ mm and $a_5 = 20$ mm.

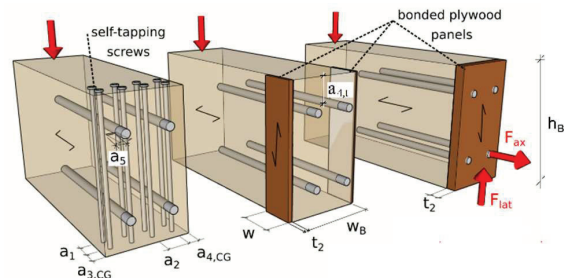


Figure 9: View of investigated reinforcement alternatives for rigid glued-in rod joints being self-tapping screws, laterally and end-grain bonded beech plywood plates

In order to grasp the load sharing between the rods with regard to both, lateral and axial forces, specifically designed test set-ups were used to measure both rod loadings with uni- and bi-axial load cells. The axial forces were measured at all rods: Bound to the size of the load cells the lateral force was however measured exclusively at the rod(s) located further from the loaded edge. The lateral force at the rod(s) placed at $a_{4,t}$ (Figure 6) was then derived from the difference of the applied and measured forces. For details see also [23]. To realize a clamped connection of the steel rods to a steel frame, comparable to a concrete connection with in-between positioned load cells, the glued-in rods were either screwed directly to the frame or connected via fitting parts. Figure 10 shows the realized test-set up for the cantilever configuration with $M/V = 1,15$. The tests were performed either in monotonic or multiple reversed loading, the latter not discussed here. The horizontal and vertical displacements at the clamped and free end of the specimens were measured, too.

Table 1: Compilation of test program for the shear force tests

designation of test	type of reinforcement	GLT width and height	position of rod along beam height	number of tests
S1	none		near (α_1)	4
			far (α_2)	3
			near + far ($\alpha_1=0,23$)	3
S1_screw	screws	80 mm x 280 mm	near (α_1)	2
			far (α_2)	1
			near + far ($\alpha_1=0,23$)	1
S1_end	end-grain plate		near (α_1)	3
			far (α_2)	2
			near + far ($\alpha_1=0,23$)	3
S3	none	160 mm x 280 mm	near (α_1)	2
			far (α_2)	2
			near + far ($\alpha_1=0,23$)	2
S3_end	end-grain plate		near (α_1)	1
			far (α_2)	1

Table 2: Compilation of test program for the cantilever tests

designation of test and M/V ratio	type of reinforcement	length of width and height of GLT in cm	GLT width and height	position of rod along beam height	number of tests
C1 (0,55)	none	60	80 mm x 280 mm	near + far (α_1 and α_2)	6
C2 (1,15)	none	120			7
C1_screw (0,55)	screws	60	80 mm x 280 mm	near + far (α_1 and α_2)	3
C2_screw (1,15)	screws	120			3
C1_lateral (0,55)	lateral panel	60	80 mm x 280 mm	near + far (α_1 and α_2)	3
C2_lateral (1,15)	lateral panel	120			3
C1_end (0,55)	end-grain plate	60	80 mm x 280 mm	near + far (α_1 and α_2)	2
C2_end (1,15)	end-grain plate	120			3
C5 (0,55)	none	60	160 mm x 280 mm	near + far (α_1 and α_2)	5
C6 (1,15)	none	120			5
C5_screw (0,55)	screws	60	160 mm x 280 mm	near + far (α_1 and α_2)	3
C6_screw (1,15)	screws	120			2
C5_lateral (0,55)	lateral panel	60	160 mm x 280 mm	near + far (α_1 and α_2)	2
C5_lateral (1,15)	lateral panel	120			2
C5_end (0,55)	end-grain plate	60	160 mm x 280 mm	near + far (α_1 and α_2)	2
C6_end (1,15)	end-grain plate	120			2
C7 (1,95)	none	200	80 x 280	near + far (α_1 and α_2)	4
C8 (1,95)	none	200	160 x 280	near + far (α_1 and α_2)	3

Additional to the full-scale beam and cantilever tests small scale tests were performed with regard to determination of the embedment strength of steel dowels of 16 mm and 20 mm diameter oriented parallel to grain in order to verify Eq. (4). These tests were aligned with EN 383 [25]. Further, the bond strength of the bond line between end-grain face of the glulam and the wide plywood panel face, so far unknown, was investigated with block shear specimens. These specimens were tested either in dry condition or after treatment in boiling water acc. to EN 14374, Annex B [26], followed by re-drying at 60°C. The tests were aligned with EN 14080 [27] but shear length had to be reduced due to excessive indentation in the GLT subjected to compression perpendicular to grain when applying the shear force.



Figure 10: Test set-up of a cantilever type GLT specimen ($b = 80$ mm) with two glued-in rods and lateral reinforcement at the clamped end by bonded beech plywood strips

6 TEST RESULTS

6.1 EMBEDMENT STRENGTH

The results of the embedment strength tests are shown in Figure 11. Despite the rather low number of specimens it is evident that the strength-density relationship given in the EC5-1-1 draft [1] is too conservative especially in the usual density range of softwood glulam. At a density of about 350 kg/m³ the minimum experimentally obtained $f_{b,k}$ values are about 5,5 N/mm² as compared to a characteristic value of about 2,5 - 3 N/mm² derived standard-wise from Eq. (4).

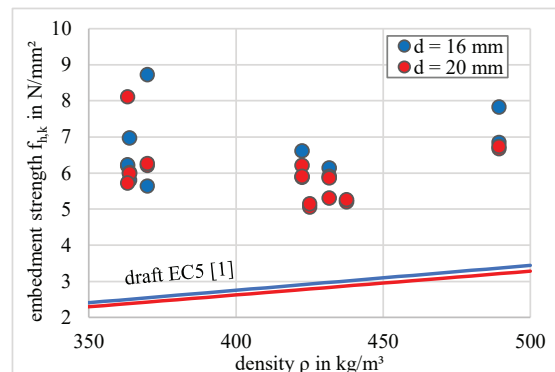


Figure 11: Test results of GLT embedment strength tests of dowels oriented parallel to grain

6.2 STRENGTH OF GLT-PLYWOOD END-GRAIN BOND LINES

Up to today end-grain bonding is considered being ineffective and of very low strength and bond line integrity. The only known approach to end-grain bonding then however of two CLT end-grain faces is pursued in the Swiss TS3 technology [28]. For bond lines between end-grain faces of GLT and plywood surfaces no shear strength values can be found in literature. Figure 12 shows the test results and further the requirement acc. to EN 14080 for fiber-parallel face bonded spruce laminations is shown. It can be seen that most of the results fulfil the requirement acc. to [27]. The obtained shear strengths varied from 3,5 - 6 N/mm² with a very high wood failure percentage of almost 100%. The difference between the higher strengths of the untreated specimens vs. the treated ones was about 20% on the mean level. So, the effect of the boiling water treatment revealed to be unexpectedly very low.

For a design of an end-grain reinforced joint (see chapt. 7) mean and minimum values of the shear strength $f_{v,b,end-grain}$ of 4,6 N/mm² and 3,5 N/mm², respectively, can be proposed tentatively.

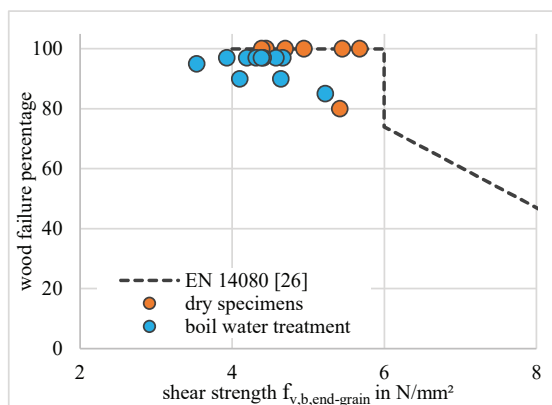


Figure 12: Bond line shear strength test results of bond lines between GLT end-grain and beech plywood panels

6.3 SHEAR FORCE TESTS

Figure 13 shows in condensed manner the results of the shear force tests for the unreinforced case (see also Figure 5) and the two reinforcement alternatives being screws and end-grain bonded plywood panels. Firstly, it can be seen that the new tests on the unreinforced joints fully confirm the former findings in literature [2; 15] that the shear force capacity increases significantly with larger distances from the loaded edge. However, most important is the finding that the reinforcement leads to extreme capacity increases vs. corresponding unreinforced configurations. Further, a significant difference between reinforcement with screws and end-grain bonded plates can be seen, whereby the latter method results throughout in higher values. It is sensible that the highest reinforcement increase is obtained for the most inconvenient rod placement with a small $a_{4,t}$ value. Here

screws and end-grain plates deliver capacity increases at the mean level by factors of 3,0 and 5,2. These capacity increases, then still large, are reduced to factors of 1,7 and 2,1 in case of a favourable high distance $a_{4,t}$. For the general joint situation with two opposite rods reinforced by screws and end-grain plates mean capacity increases by factors of 1,8 and 2,6 were observed.

Both reinforcement alternatives produce extremely differing stiffnesses and damage evolutions as shown in Figure 14. At very low loads the unreinforced and both reinforced joint configurations reveal comparable stiffnesses in lateral direction. In case of screw reinforcement the stiffness gets highly nonlinear at very low loads. Contrary, the stiffness of the end-grain reinforced joint remains strictly linear up to about 50% of ultimate load and beyond this threshold a progressive nonlinear stiffness evolution starts. The failure mechanisms differ as follows. In case of screw reinforcement similar as with unreinforced joints splitting parallel to fiber occurs starting at the end-grain face at the rod positions closer to the loaded edge. However, the crack propagation is strongly delayed by the screw forces normal to the crack faces. At ultimate load and very large deformations in the rod embedment area a sudden load drop due to cracking of the GLT parallel to grain at the screw reinforcement occurs. Contrary in case of end-grain plate reinforced joints the nonlinearity without any crack formation is induced by deformations of the rod embedment area in the plywood. At ultimate load finally also splitting in combination with either a tensile failure in the net cross-section of the panel (see Figure 17) or a failure of the bond line between the GLT end-grain and reinforcement panel occurs. Details of reinforcements with laterally bonded plywood stripes which delivered comparable capacity gains as the screw reinforcements are not discussed here, as their range of application is limited to rather slender beams because of an expressed decline of the reinforcement effect with increasing width of the GLT.

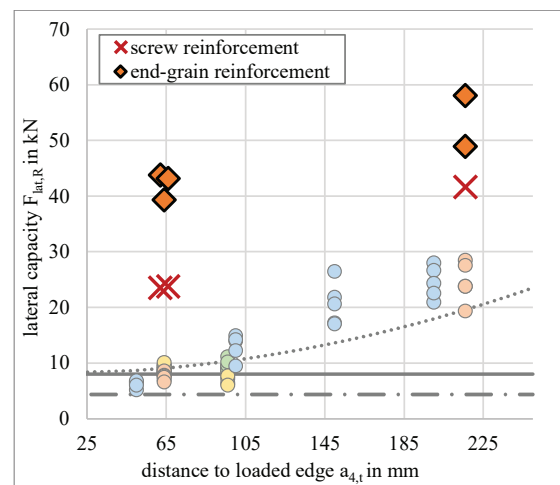


Figure 13: Test results of quasi pure laterally loaded steel rods glued in GLT parallel to fiber without and with reinforcements by i) self-tapping screws or ii) end-grain bonded plywood

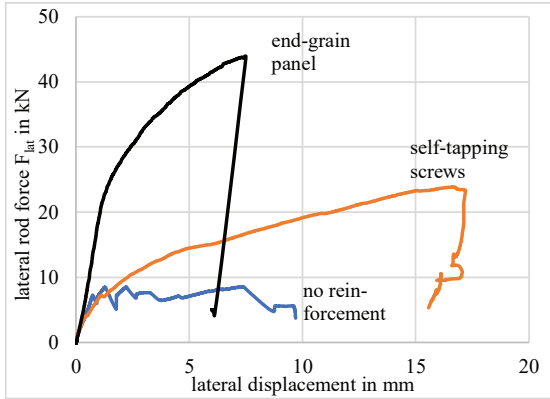


Figure 14: Stiffness evolution of quasi pure laterally loaded steel rods glued in GLT parallel to grain without and with reinforcement of self-tapping screws or an end-grain bonded plywood panel

6.4 CANTILEVER TESTS

A brief compilation of the empiric ultimate axial ($F_{ax,u}$) and lateral ($F_{lat,u}$) forces on the mean level is shown in Figure 15. On the left side the results of the shorter ($M/V = 0,55$) and on the right side the results of the longer ($M/V = 1,15$) cantilever beams are given. It can be seen, that the capacity gain of reinforced vs. unreinforced joints is decreasing with higher moment to shear force ratios. For a quantification in rough manner the capacities of the different reinforcement alternatives are lumped. At the short cantilevers the capacity gains at $F_{ax,u}$ and $F_{lat,u}$ closely resembling are denoted by factors of 1,7 – 1,8. At the long cantilevers the reinforcement gain of $F_{ax,u}$ and $F_{lat,u}$ decreases to an equal factor of about 1,3. This fact results from the already very high axial force capacity of the unreinforced joints at the higher M/V -ratio resulting in a mean withdrawal strength of $f_w = 5,2 \text{ N/mm}^2$. This narrows the potential for a capacity increase as i) f_w is limited to maximally about 7 N/mm^2 in pure axial loading and ii) the yield capacity of the steel rod itself is $100,4 \text{ kN}$ for the given configuration.

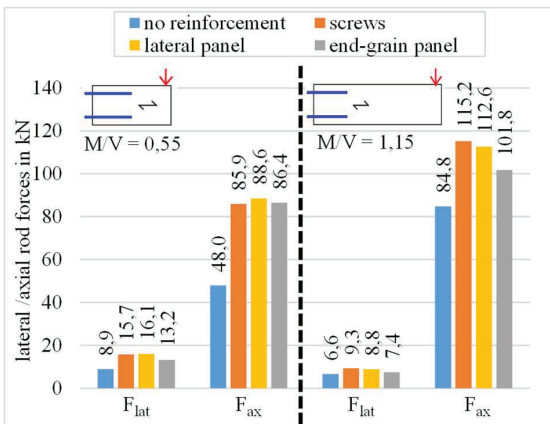


Figure 15: Test results of cantilever type specimens with clamped glued-in steel rod connections without or with reinforcement

Figure 16 shows the ultimate capacities of all tests with pure axial, pure lateral and combined moment and shear loading. For comparison the interaction line for the characteristic forces of unreinforced joints acc. to draft EC5-1-1 [1] as derived from Eqs. (1) to (5) is given, too. Similarly, as in case of lateral loading (see Figure 13) the enormous capacity gains throughout all possible $F_{ax} - F_{lat}$ force combinations enabled by the investigated joint reinforcements are evident.

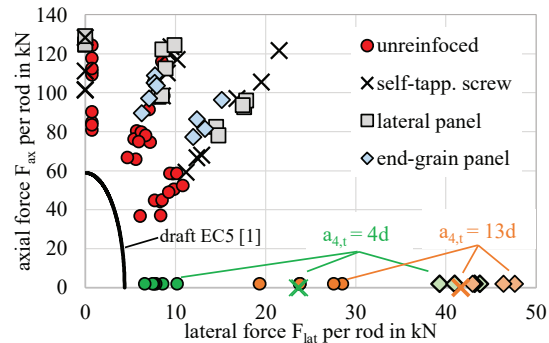


Figure 16: Compilation of test results from pure axial, pure lateral and combined loaded glued-in rod joint configurations without and with reinforcements

7 DESIGN PROPOSAL FOR END GRAIN REINFORCED RIGID JOINTS

Riberholt [15], [17] holds the merit for firstly presenting experimental tests with rods glued-in parallel to grain and loaded laterally as well as by combined moment and shear force action. He observed splitting as a weakness of the joints when either the beams were very slim or the rod was close to the loaded beam edge. Based on the test results the lateral rod capacity of unreinforced joints and for an eccentricity of $e = 0 \text{ mm}$ was then proposed as

$$F_{lat,unrein,Rk} = f_{h1,k} \cdot d \cdot \sqrt{\frac{2 \cdot M_{y,Rk}}{f_{h1,k} \cdot d}} \quad (6)$$

$$= \sqrt{2} \cdot \sqrt{f_{h1,k} \cdot d \cdot M_{y,Rk}}$$

Eq. (6) conforms to draft EC5-1-1 [1], here Eq. (2b), and mirrors the case of a single plastic hinge in the timber dowel-jointed to a thin steel plate (Note: Eq. (6) differs from Eq. 8.9 in EC5-1-1 [29] by the prefactor of 1,15 and the missing rope effect consideration).

To overcome the joint splitting deficiency, Riberholt investigated a reinforcement by a 9 mm birch plywood panel glued-on the GLT end-grain. Based hereon Eq. (6) was then extended [17] to the case of an end-grain reinforcement as (see [23])

$$F_{lat, reinf, Rk} = \left[\left(\sqrt{\frac{2 \cdot M_{y, Rk}}{f_{h1, k} \cdot d}} - t_p \cdot \left(\frac{f_{h2, k}}{f_{h1, k}} - 1 \right) - t_p \right) \cdot f_{h1, k} + t_p \cdot f_{h2, k} \right] \cdot d \quad (7)$$

where

- $f_{h1, k}$ embedment strength of spruce (rod parallel to grain and loaded laterally) similar to Eq. (4)
- $f_{h2, k}$ embedment strength of the plywood panel as $f_{h2, k} = 0,11 \cdot (1 - 0,01 \cdot d_{drill}) \cdot \rho_{k, ply}$ [1]
- $M_{y, Rk}$ yield moment of the steel rod similar to Eq. (3)
- t_p thickness of the plywood panel
- d steel rod diameter
- d_{drill} the drill diameter of the hole in the timber part

Equation (7) describes a failure mode of a single plastic hinge in the GLT or of two yield hinges in case the glued-on end-grain panel is thick. If the embedment strength of the GLT parallel to grain is neglected ($f_{h1, k} = 0$) in a conservative design approach as being roughly 20 times smaller as compared to $f_{h2, k}$, the lateral capacity acc. to Eq. (7) results in

$$F_{lat, emb, reinf, Rk} = f_{h2, k} \cdot d \cdot t_p \quad (8)$$

and mirrors a pure dependency of the joint capacity with the panels embedment strength.

For the investigated specimen configuration, the lateral force resistances acc. to Eqs. (6) to (8) result in

$$F_{lat, Rk, unreinf} = 4,4 \text{ kN},$$

$$F_{lat, reinf, Rk} = 19,9 \text{ kN and}$$

$$F_{lat, emb, reinf, Rk} = 19,2 \text{ kN}$$

where $f_{h1, k} = 2,8 \text{ N/mm}^2$, $\rho_{k, GLT} = 430 \text{ kg/m}^3$, $d_{drill} = 20 \text{ mm}$, $f_{h2, k} = 60 \text{ N/mm}^2$ ($\rho_{k, panel} = 680 \text{ kg/m}^3$); $M_{y, Rk} = 210 \text{ kNmm}$ (with $f_{u, k} = 800 \text{ N/mm}^2$, $d_e = 13,54 \text{ mm}$); $d = 16 \text{ mm}$; $t_p = 20 \text{ mm}$, e is assumed to be 0.

In addition to the embedment / plastic hinge resistance capacity of the end-grain panel the shear force transfer of the plate bonded to the GLT end-grain face has to be verified for the bond line interface (Figure 17a). Although the panel is bonded over the entire end-grain face area an uneven shear stress distribution has to be considered. In a first approach a roughly triangular distribution can be assumed or as proposed here in conservative manner an effective shearing length of

$$h_{b, eff} = 2 \cdot a_{4, t}$$

is chosen. The width of the effective bond area is assumed to be

$$w_{b, eff} = 5 \cdot d_{rod},$$

which is the minimum spacing between rods acc. to [1].

The characteristic lateral capacity of the bonded GLT-panel interface is then given by

$$F_{lat, bond, Rk} = h_{b, eff} \cdot w_{b, eff} \cdot f_{v, b, end-grain, k} \quad (9)$$

where

- $f_{v, b, end-grain, k}$ characteristic bond line shear strength of GLT vs. plywood panel

According to the test results given above for the shear strength with $f_{v, b, end-grain, k} = 3,5 \text{ N/mm}^2$, the joint bond capacity for a single rod in the given case is

$$F_{lat, bond, Rk} = 2 \cdot 64 \text{ mm} \cdot 5 \cdot 16 \text{ mm} \cdot 3,5 \text{ N/mm}^2 = 35,8 \text{ kN}.$$

Further the tension capacity of the panel net cross-section in direction of the shear force, being in general parallel to beam height, has to be verified as (see Figure 17b)

$$F_{lat, panel, t, Rk} = t_p \cdot (w_{b, eff} - d_{drill}) \cdot f_{t, plate, k} \quad (10)$$

where

- $f_{t, plate}$ characteristic tensile capacity of the plywood panel, assumed as $f_{t, plate, k} = 30 \text{ N/mm}^2$ acc. to [8].

Eq. (10) then results for the plywood plate used in the tests in a tensile capacity of

$$F_{lat, panel, t, Rk} = 20 \text{ mm} \cdot (80 \text{ mm} - 20 \text{ mm}) \cdot 30 \text{ N/mm}^2 = 36,0 \text{ kN}$$

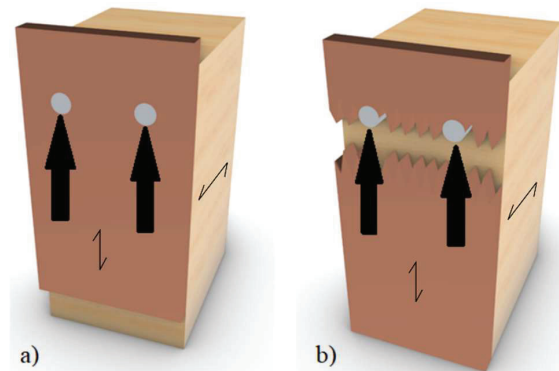


Figure 17: Failure mechanisms of the end-grain bonded plywood reinforcement a) bond line shear failure b) tensile failure

Summarizing: for the design of a glued-in rod joint with an end-grain reinforcement the following conditions of the lateral force resistance have to be satisfied:

$$F_{lat, Ek} \leq F_{lat, Rk} = \min \begin{cases} F_{lat, emb, reinf, Rk} & \text{Eq. (8)} \\ F_{lat, bond, Rk} & \text{Eq. (9)} \\ F_{lat, panel, t, Rk} & \text{Eq. (10)} \end{cases} \quad (11)$$

Eq. (11) results as outlined in capacities of 19,2 kN, 35,8 kN and 360 kN, respectively. The minimum resistance of 192 kN results from the embedment failure (Eq.(8)) of the glued-on plywood panel. It is apparent that the above derived characteristic design resistance of the joint is significantly lower as compared to the test results. The minimum test result of a laterally loaded end-grain reinforced joint with $a_{4, t} = 4 \cdot 16 \text{ mm} = 64 \text{ mm}$ is by a factor of 2 higher than the result of the embedment design equation. The reason therefore can be explained from the load displacement curve (see Figure 14), which shows that the stiffness develops increasingly non-linear beyond a shear force of about 20 kN which conforms roughly to the characteristic embedment capacity of the bonded plywood panel. A more profound discussion of this altogether with an improved design equation for the

lateral joint capacity resulting from plate embedment and rod yielding is given separately.

8 CONCLUSIONS

In rigidly clamped unreinforced glulam joints made with glued-in rods the connection capacity is widely determined by the lateral loads resulting from the shear force. The lateral rod force leads to tensile stresses perpendicular to grain and hence to premature splitting which undermines the activation of the axial rod capacity potential. Reinforcements of glued-in rod joints are not considered in the draft of the new Eurocode 5 [1]. The presented research on glued-in rods subjected to pure lateral and combined moment-shear-force loading proved that reinforcements by self-tapping screws as well as by laterally and end-grain bonded plywood panel(s) enable the full utilization of the axial rod withdrawal capacity. End-grain reinforcements of the GLT beam by bonding a plywood panel with a resorcinol adhesive so far not used in timber engineering at all seems to be superior as compared to self-tapping screws because of a lower result scatter. It further provides the potential to reduce the edge distances of the glued-in rods. On the other hand, self-tapping screws which enable high capacity gains, too, are very easy to install and highly apt for reinforcements of existing unreinforced joints.

Laterally bonded plywood strips are comparably efficient as self-tapping screws and end-grain bonded plates but are confined to rather narrow GLT cross-sections due to the limited reinforcement spread.

Auxiliary investigations related to derivation of design equations revealed that the embedment strength of dowel-type-fasteners, here rods, oriented parallel to grain is specified much too conservative in the new draft of Eurocode 5 [1]. Similarly, the missing consideration of the distance to the loaded edge in the draft EC5 design equations for the lateral rod capacity lead in most cases to overly conservative resistances of unreinforced joints. Regarding end-grain reinforcements by plywood made from hardwoods the test results exceed a formerly literature proposed design equation by a factor of two. A new design approach in order to represent the true potential of this promising jointing technology is presently being developed.

ACKNOWLEDGEMENT

The partial support of this work by Deutsche Forschungsgemeinschaft (DFG, German Research Foundation) to project RP3 of IntCDC (Integrative Computational Design and Construction for Architecture) and Germany's Excellence Strategy is gratefully acknowledged.

REFERENCES

- [1] prEN 1995-1-1 (2022) working draft (formal enquiry): Design of timber structures - Part 1-1: General and rules for buildings (CEN/TC 250/SC 5, N 1650). CEN, Brussels, Belgium, 2022.
- [2] Blaß H.J.; Laskewitz B.: Glued-in Rods for Timber Structures – Effect of distance between rods and between rods and timber edge on the axial strength; Versuchsanstalt für Stahl, Holz und Steine – Abteilung Ingenieurholzbau; University Fridericiana Karlsruhe, 2001.
- [3] Ehlbeck J., Görlacher R., Werner H.: Determination of perpendicular-to-grain tensile stresses in joints with dowel-type fasteners; a draft proposal for design rules, *CIB-W18A proceedings*, Berlin, Germany, 1989.
- [4] Wirth C.: High-bay warehouse in wood – new application for wood. In: Conference Proceedings of 13. *Internationales Holzbau-Forum IHF*, Garmisch Partenkirchen, Germany, 2007.
- [5] Aicher S, Herr J: Investigations on high strength glulam frame corners with glued-in steel connectors. In: Proceedings of 5th World Conference on Timber Engineering, pp. 273-280, Montreux, Switzerland, 1998.
- [6] Edlund G.: I limträ inlimmad skruer. Svenska Träforskningsinstitutet, Serie B nr. 333, STFI Svenska Träforskningsinst, 1975.
- [7] Aicher S.; Stapf G.: Glued-in rods – state of the art – influencing factors, test results, approvals, adhesive standardisation, dimensioning and design rules (in German). In: Conference Proceedings of 23. *Internationales Holzbau-Forum IHF*, Garmisch Partenkirchen, Germany, 2017.
- [8] DIN 1052:2004: Design of timber structures - General rules and rules for buildings. German Institute for Standardization, Berlin, Germany, 2004.
- [9] DIN EN 1995-1-1/NA:2013: National Annex - Nationally determined parameters - Eurocode 5: Design of timber structures - Part 1-1: General - Common rules and rules for buildings. German Institute for Standardization, Berlin, Germany, 2013.
- [10] German Technical Approval Z-9.1-705: 2K-EP-adhesive WEVO special resin EP 32 S with hardener B22 TS, WEVO-Chemie GmbH Ostfildern-Kemnat. DIBt, Berlin, Germany, 2022.
- [11] German Technical Approval Z-9.1-707: 2K-PUR-adhesive LOCTITE CR421 PURBOND for bonding steel rods into timber structures, Henkel & Cie. AG, Sempach Station, Switzerland. DIBt, Berlin, Germany, 2021.
- [12] German Technical Approval Z-9.1-778: 2K-EP-adhesive GSA-resin and GSA-hardener for bonding of steel rods into wooden parts, neue Holzbau AG, Lungern, Switzerland. DIBt, Berlin, Germany, 2021

- [13] German Technical Approval Z-9.1-902: Connections with glued-in steel rods into timber parts with 2K-EP-adhesive (injection mortar) Hilti HIT-RE 500 V4, Hilti Germany, Kaufering. DIBt, Berlin, Germany, 2021
- [14] EN 17334:2021: Glued-in rods in glued structural timber products - Testing, requirements and bond shear strength classification. CEN, Brussels, Belgium, 2021.
- [15] Riberholt, H.: Bolte Indlimet I Limtrae; Technical University of Denmark; Structural Research Laboratory, Rapport Nr. R 83; 1977.
- [16] Möhler, K; Hemmer, K: Tests with glued-in threaded steel rods; Lehrstuhl für Ingenieurholzbau und Baukonstruktionen, University Fridericiana Karlsruhe, Germany, 1981.
- [17] Riberholt, H: Glued bolts in glulam – proposal for CIB code; *International Council for Building Research Studies and Documentation – Working Commission W18A/21-7-2 – Timber Structures*; Meeting 21; Vancouver Island, Canada, 1988.
- [18] Johansen K.W.: Theory of Timber Connections. *International Association for Bridge and Structural Engineering*, Vol. 9, pp. 249-262, 1949.
- [19] Eurocode 5 draft (2021). informal enquiry: prEN 1995-1-1: Design of timber structures - Part 1-1: General and rules for buildings (CEN/TC 250/SC 5 N 1488). Brussels, Belgium: CEN.
- [20] Aicher S.; Leitschuh N. und Hezel J.: „Stuttgarter Holzbrücke“, Research Report EFRE research project, Nr. 051203. MPA University of Stuttgart, 2015.
- [21] Hezel J., Aicher S.: Die Stuttgarter Brücke – ein neuer Robustheitsansatz. Proceedings 4. International Days on Timber Bridges, IHB Ostfildern, Germany, 2016.
- [22] Aicher S., Simon K.: Rigid glulam joints with glued-in rods subjected to axial and lateral force action. In: Proceedings International Network on Timber Engineering and Research (INTER), Meeting 54, pp. 113-128, Karlsruhe, Germany, 2021.
- [23] Simon K., Aicher S.: Reinforced rigid glulam joints with glued-in rods subjected to axial and lateral force action. In: Proceedings *International Network on Timber Engineering Research (INTER)*, Meeting 55, pp. 185-201, Bad Aibling, Germany, 2022.
- [24] Hezel J, Aicher S, Helbig T: Integral, bonded Timber-Concrete-Abutment-Connection (in German), In Proceedings of 3rd Stuttgarter Holzbau-Symposium, pp. 97-107, Stuttgart, Germany, 2015.
- [25] EN 383:2007: Timber Structures –Test methods – Determination of embedment strength and foundation values for dowel type fasteners. CEN, Brussels, Belgium, 2007.
- [26] EN 14374:2004: Timber structures - Structural laminated veneer lumber – Requirements. CEN, Brussels, Belgium, 2004.
- [27] EN 14080:2013: Timber structures - Glued laminated timber and glued solid timber – Requirements. CEN, Brussels, Belgium, 2013.
- [28] Franke S., Zöllig S.: TS3 – A New Technology for Efficient Timber Structures. In: *Current Trends for Civil & Structural Engineering* 4(4): 2020.
- [29] EN 1995-1-1 (2010): Design of timber structures - Part 1-1: General - Common rules and rules for buildings, CEN, Brussels, Belgium, 2010.